Iso-surfaces and their propagation in turbulent premixed combustion and other flows

By S. H. Kim AND R. W. Bilger†

1. Motivation and objectives

The study of the behavior of iso-scalar surfaces is crucial in understanding turbulent mixing and combustion. Iso-surfaces in turbulent flows are quite complicated due to stretching and folding by random velocity fluctuations with a broadband spectrum of time and length scales (Candel & Poinsot 1990; Trouve & Poinsot 1994; Vervisch *et al.* 1995). Increased surface area and scalar gradients due to the turbulent motions result in the enhanced mixing of the scalar. Overall reaction rates in turbulent nonpremixed combustion increase with the turbulent mixing rate, when there is little local extinction. The propagation of iso-surfaces is of critical importance in turbulent premixed combustion, in which the flame fronts can be defined as iso-surfaces of a reactive scalar.

Propagation of the reaction fronts in turbulent flows can be characterized by the Damköhler number, Da, defined as the ratio of turbulent time scale to chemical one, τ_t/τ_c (Damköhler 1940). In the high Da limit, in which chemical reactions are much faster than all turbulent time scales, turbulence does not disturb the inner structure of the reaction fronts but does wrinkle the reaction fronts. The propagation of the reaction fronts is then characterized by the laminar propagation speed and the increased total front surface area due to turbulent wrinkling. In the low Da limit, where all turbulent time scales are faster than chemical ones, the propagation of the reaction fronts is primarily determined by turbulent transport. In the intermediate Da, large scale eddies, the time scales of which are slower than chemical ones, wrinkle the reaction fronts, while small scale eddies, the time scales of which are faster than chemical ones, disturb the reaction fronts.

In the low and intermediate Da regimes, the propagation of the reaction fronts may not be well characterized by quantities on *one* characteristic surface, as has been done in previous studies. In this paper, we study the propagation of iso-scalar surfaces in turbulent flows using a new analysis method that gives more detailed description of the iso-surface propagation. Direct numerical simulation (DNS) data for statistically one dimensional turbulent premixed flames and isothermal reaction front propagation are analyzed using the proposed method. Application to conserved scalar mixing is also presented.

2. Mathematical formulation

2.1. *Basic concepts*

The kinematic and dynamic properties of iso-surfaces can be characterized by the surface density function and by the displacement speed of the iso-surfaces. Based on these

† The University of Sydney, Australia.

quantities, we present expressions for the mass flux through the iso-surfaces. It is demonstrated in the subsequent sections that these concepts are useful in characterizing the propagation of premixed flames as well as the entrainment process.

The rate of displacement $\mathbf{U}_\phi$ of a constant property surface with scalar $\phi = \varphi$ is given by

$$\mathbf{U}_\phi = \frac{-\mathbf{n}\frac{\partial \phi}{\partial t}}{|\nabla \phi|}, \tag{2.1}$$

where $\mathbf{n} = \nabla\phi/|\nabla\phi|$ is the unit vector normal to the constant property surface, positive in the direction of increasing ϕ. The velocity of the surface relative to the fluid $\mathbf{u}_\phi$ is given by (Gibson 1968; Pope 1988)

$$\mathbf{u}_\phi = \mathbf{U}_\phi - \mathbf{U} = \frac{-\mathbf{n}\frac{D\phi}{Dt}}{|\nabla \phi|}, \tag{2.2}$$

where $\mathbf{U}$ is the fluid velocity and $\frac{D\phi}{Dt} = \frac{\partial \phi}{\partial t} + \mathbf{U}\cdot\nabla\phi$ is the substantial or Stokes derivative of ϕ. The evolution equation for ϕ can then be written as

$$\frac{D\phi}{Dt} = -|\nabla\phi|(\mathbf{n}\cdot\mathbf{u}_\phi) = -|\nabla\phi|u_\phi, \tag{2.3}$$

where u_ϕ is the magnitude of $\mathbf{u}_\phi$.

The fine-grained surface density, Σ_φ, of the surface with $\phi = \varphi$ is given by (Pope 1990; Vervisch *et al.* 1995)

$$\Sigma_\varphi = |\nabla\phi|\delta(\phi - \varphi), \tag{2.4}$$

where $\delta(\phi - \varphi)$ is the Dirac delta function. Σ_φ measures the infinitesimal of surface-to-volume ratio of the iso-surfaces. The integration of Σ_φ over the volume V gives total area of the instantaneous iso-surfaces in V. Averaging (2.4) gives the mean surface density:

$$\overline{\Sigma}_\varphi = \langle|\nabla\phi||\phi(\mathbf{x},t) = \varphi\rangle P(\varphi;\mathbf{x},t), \tag{2.5}$$

where the angle brackets with the vertical bar denote the average, conditional on the condition to the right of the vertical bar. $P(\varphi;\mathbf{x},t)$ is the probability density function (PDF) of ϕ at the point $\mathbf{x}$ at time t.

The fine grained mass flow rate per unit volume $\dot{m}'''_\varphi$ through the iso-surface with $\phi = \varphi$ (positive in the direction of $\nabla\phi$) is given by

$$\dot{m}'''_\varphi = -\rho\Sigma_\varphi u_\phi = \rho\frac{D\phi}{Dt}\delta(\phi - \varphi). \tag{2.6}$$

The ensemble average of this is the average mass flow rate of the fluid per unit volume through the iso-surface, R_φ, positive in the direction of increasing ϕ, and is given by

$$R_\varphi(\mathbf{x},t) = \langle\rho\frac{D\phi}{Dt}|\phi(\mathbf{x},t) = \varphi\rangle P(\varphi;\mathbf{x},t). \tag{2.7}$$

A total mass flux through the iso-ϕ surface is obtained by

$$\Gamma_\varphi(\mathbf{y},t) = \int_{m_1}^{m_2} R_\varphi(\mathbf{x},t)w dm, \tag{2.8}$$

where m is the coordinate along the integration path. m_1 and m_2 correspond, respectively, to $\widetilde{\phi}_{min}$ and $\widetilde{\phi}_{max}$, where $\widetilde{\phi}_{min}$ and $\widetilde{\phi}_{max}$ are the minimum and maximum of $\widetilde{\phi}$ along the integration line, respectively. It is assumed in (2.8) that $\widetilde{\phi}$ is monotonically increasing from $\widetilde{\phi}_{min}$ to $\widetilde{\phi}_{max}$ along the integration path. $\mathbf{y}$ represents the location of the integration

path. w is a nondimensional weighting factor. A characteristic propagation speed of the iso-surfaces can be defined as

$$S_\varphi(\mathbf{y},t) = \frac{\Gamma_\varphi(\mathbf{y},t)}{\rho_c}, \tag{2.9}$$

where ρ_c is the characteristic density. Similarly, the mean wrinkled surface area ratio is given by

$$A_\varphi(\mathbf{y},t) = \int_{m_1}^{m_2} \overline{\Sigma}_\varphi(\mathbf{x},t) w dm. \tag{2.10}$$

A_φ measures the increase of the mean area of the instantaneous iso-surfaces due to turbulent stretching and folding. The choice of the integration path m and the weighting factor w depends on the case.

2.2. *Conserved scalar mixing*

The conserved scalar ξ obeys

$$\rho \frac{D\xi}{Dt} = \nabla \cdot (\rho D_\xi \nabla \xi), \tag{2.11}$$

where Fickian diffusion is assumed with a molecular diffusivity, D_ξ. (2.7) then becomes

$$R_\eta(\mathbf{x},t) = \rho_\eta M_\eta(\mathbf{x},t) P(\eta;\mathbf{x},t) = \frac{\partial \rho_\eta N_\eta P(\eta)}{\partial \eta}. \tag{2.12}$$

Here M_η is the conditional average diffusion defined as

$$M_\eta \equiv \frac{1}{\rho_\eta} \langle \nabla \cdot (\rho D_\eta \nabla \xi) \, | \xi = \eta \rangle. \tag{2.13}$$

The conditional average density and the conditional average scalar dissipation are, respectively, defined as

$$\rho_\eta \equiv \langle \rho | \xi = \eta \rangle \tag{2.14}$$

$$N_\eta \equiv \frac{1}{\rho_\eta} \langle \rho \nabla \xi \cdot \nabla \xi | \xi = \eta \rangle. \tag{2.15}$$

Derivation of the relationship between the conditional diffusion and the conditional dissipation can be found in Klimenko & Bilger (1999). The $(\mathbf{x},t)$ dependence of these quantities and of the PDF are omitted to improve clarity.

The total mass flux through the iso-ξ surfaces is given by

$$\Gamma_\eta(\mathbf{y},t) = \int_{m_1}^{m_2} \rho_\eta M_\eta P(\eta) w dm. \tag{2.16}$$

In conserved scalar mixing, the conditional mean density through the mixing layer can be used to obtain the characteristic propagation speed. The characteristic propagation speed is then given by

$$S_\eta(\mathbf{y},t) = \frac{\Gamma_\eta(\mathbf{y},t)}{\rho_\eta^*}, \tag{2.17}$$

where

$$\rho_\eta^* = \frac{\int_{m_1}^{m_2} \rho_\eta w dm}{\int_{m_1}^{m_2} w dm}. \tag{2.18}$$

The wrinkled surface ratio can be written as

$$A_\eta(\mathbf{y},t) = \int_{m_1}^{m_2} \langle |\nabla \xi| | \xi = \eta \rangle P(\eta) w dm. \tag{2.19}$$

2.3. *Isothermal reaction fronts and turbulent premixed flames*

The reaction progress variable C in reaction fronts propagation is defined so as to obey the equation

$$\rho \frac{DC}{Dt} = \nabla \cdot (\rho D_C \nabla C) + \rho W_C, \tag{2.20}$$

where W_C is the reaction rate per unit mass and D_C is the molecular diffusivity for the progress variable. This yields

$$R_\zeta(\mathbf{x},t) = \left(\rho_\zeta M_\zeta + \langle \rho W_C | \zeta \rangle\right) P(\zeta), \tag{2.21}$$

where

$$M_\zeta = \frac{1}{\rho_\zeta} \langle \nabla \cdot (\rho D_C \nabla C) | \zeta \rangle. \tag{2.22}$$

ζ is the sample space variable for C. $\rho_\zeta \equiv \langle \rho | \zeta = C \rangle$ is the conditional average density.

R_ζ is the apparent turbulent burning rate per unit volume in turbulent premixed flames. Note the contribution of the conditional diffusion term M_ζ. (2.21) shows that the apparent burning rate, i.e. consumption rate of fresh mixture, can depend on the value of ζ chosen. Integration of R_ζ across the flame brush gives the total mass flux through the iso-C surfaces:

$$\Gamma_\zeta(\mathbf{y},t) = \int_{m_1}^{m_2} \left(\rho_\zeta M_\zeta + \langle \rho W_C | \zeta \rangle\right) P(\zeta) w dm. \tag{2.23}$$

A turbulent burning velocity can be defined as

$$S_T(\zeta,\mathbf{y},t) = \frac{\Gamma_\zeta(\mathbf{y},t)}{\rho_u}, \tag{2.24}$$

where ρ_u is the unburnt density. The wrinkled surface ratio can be written as

$$A_T(\zeta,\mathbf{y},t) = \int_{m_1}^{m_2} \langle |\nabla C| | C = \zeta \rangle P(\zeta) w dm. \tag{2.25}$$

3. Direct numerical simulations

Direct numerical simulations are carried out to demonstrate the usefulness of the proposed concepts in understanding iso-surface propagation in turbulent flows. The fully compressible Navier-Stokes equations are solved:

$$\frac{\partial \rho}{\partial t} + \frac{\partial \rho u_i}{\partial x_i} = 0 \tag{3.1}$$

$$\frac{\partial \rho u_i}{\partial t} + \frac{\partial}{\partial x_j}(\rho u_i u_j) = -\frac{\partial p}{\partial x_i} + \frac{\partial \tau_{ij}}{\partial x_j} + \rho f_i \tag{3.2}$$

$$\frac{\partial \rho e}{\partial t} + \frac{\partial}{\partial x_j}[(\rho e + p) u_i] = \frac{\partial u_j \tau_{ij}}{\partial x_i} + \frac{\partial}{\partial x_i}(\lambda \frac{\partial T}{\partial x_i}) + \rho Q \omega_\phi + \rho f_i u_i \tag{3.3}$$

$$\frac{\partial \rho \phi}{\partial t} + \frac{\partial}{\partial x_j}(\rho u_i \phi) = \frac{\partial}{\partial x_i}(\rho D \frac{\partial \phi}{\partial x_i}) + \rho \omega_\phi, \tag{3.4}$$

where

$$\rho e = \frac{1}{2}\rho u_i u_i + \frac{p}{\gamma - 1} \tag{3.5}$$

$$\tau_{ij} = \mu \left(\frac{\partial u_i}{\partial x_j} + \frac{\partial u_j}{\partial x_i} - \frac{2}{3}\delta_{ij}\frac{\partial u_k}{\partial x_k} \right). \tag{3.6}$$

p is pressure, e is the sensible internal energy, ω_ϕ is the chemical reaction rate of the scalar ϕ, Q is a heat release parameter, f_i is an external forcing term. The thermal conductivity λ and the diffusion coefficient D are given as

$$\lambda = \mu c_p / Pr \text{ and } D = \mu/(\rho Sc), \tag{3.7}$$

where c_p is the specific heat at constant pressure. The dynamic viscosity μ is given as

$$\mu = \mu_u (T/T_u)^n. \tag{3.8}$$

The Prandtl number Pr and the Schmidt number Sc are set to be 0.7. The gas mixture is assumed to be a perfect gas with a specific heat ratio of γ=1.4. The equations are integrated using a low storage fourth order Runge-Kutta method with a sixth order compact finite difference scheme for spatial discretization (Kennedy *et al.* 2000; Lele 1992).

3.1. *Conserved scalar mixing*

Passive conserved scalar mixing in forced, homogeneous isotropic turbulence is simulated: $\omega_\phi = 0$. Linear forcing of Lundgren (Lundgren 2003; Rosales & Meneveau 2005) is used:

$$f_i = A_f u_i, \tag{3.9}$$

where the forcing constant, A_f, is set to be 0.3 here. The Reynolds number based on Taylor micro scale is 56. The passive conserved scalar field is periodic in the x_2 and x_3 directions, while the Dirichlet condition is used for the x_1 direction. The initial scalar profile is given by

$$\overline{\xi} = 0.5\left[1 + \mathrm{erf}(0.5x_1/\Delta_0)\right], \tag{3.10}$$

where x_1 is set to be zero at the center of the computational domain. Δ_0 is set to be $0.01L$, where L is the characteristic length of the domain. Computation was done until the boundary condition in the x_1 direction does not influence the solution. The equations are solved on 256×128×128 grid points.

3.2. *Isothermal reaction fronts*

Reaction front propagation in homogeneous turbulence is simulated. The turbulence field is the same as that of the conserved scalar mixing case. The reaction rate is given by

$$\omega_c = A(1 - C)\exp\left(-\frac{\beta}{\alpha C}\right), \tag{3.11}$$

where A is a pre-exponential factor. C is the reaction progress variable. $\alpha = 5$ and $\beta = 4$. The front is isothermal in the sense that $Q = 0$. The underlying flow field is the same as that for passive conserved scalar mixing. The whole flow and scalar fields are shifted after a few time steps to maintain the fronts in the center of the computational domain. The scalar field is initialized using the laminar front solution with the front propagation speed S_L and the characteristic thickness l_F. The Damkohler number based on $u'/S_L = 17.67$ and $l/l_F = 3.3$ is 0.19.

	u'/s_L	l/l_F	Da	Ka	Re_λ
PF1	13.8	3.9	0.28	14	95
PF2	19.5	2.75	0.14	28	95

TABLE 1. Characteristics of the simulated premixed flames (u': rms initial turbulent velocity, l: initial integral length scale, S_L: laminar flame speed, l_F: flame thickness based on the maximum temperature gradient, Da$\equiv S_L l/(u' l_F)$, Ka$\equiv D_u^2/(S_L l_K)^2$, l_K: Kolmogorov length scale, D_u: unburned mixture diffusivity, Re_λ: Reynolds number based on the Taylor scale).

3.3. *Premixed flames*

The simulated flames are statistically one dimensional premixed flames propagating in decaying homogeneous turbulence. The reaction rate is given by

$$\omega_{Y_R} = A Y_R \exp\left(-\frac{T_a}{T}\right), \tag{3.12}$$

where Y_R is the mass fraction of the deficient species in the reactant. The activation temperature T_a is set to be $4T_b$, where T_b is the burned gas temperature. The heat release parameter Q is chosen such that the density ratio between unburned and burned gas is equal to 6. The reaction progress variable is defined here as $C = 1 - Y_R$.

A non-reflecting boundary condition is used for the x_1 direction, while the x_2 and x_3 directions are periodic (Poinsot & Lele 1992). The equations are solved on $512\times256\times256$ grid points. Initial turbulence is homogeneous and isotropic. The characteristics of the premixed flame are shown in Table 1.

4. Results

In the present DNS data base, the integration direction and the weight factor are $m = x_1$ and $w = 1$, respectively. The line integrated quantities, Γ_φ and A_φ, have no dependence on the spatial coordinate.

4.1. *Conserved scalar mixing*

Figure 1 shows total mass flux through the iso-ξ surfaces, Γ_η, at several time instants. In the present case, Γ_η is essentially the same as S_η. During the initial development, $\tau(\equiv tl/u') < 1$, Γ_η increases with time due to increased surface area. Γ_η then shows a weak dependence on time for $\tau > 1$. Γ_η is skew-symmetric about $\eta = 0.5$, suggesting that the entrainment for high and low values of η is in the opposite direction. In stationary homogeneous turbulence, the solution of the mean conserved scalar $\overline{\xi}$ can be written as

$$\overline{\xi} = 0.5\left[1 + \mathrm{erf}(0.5x_1/(D_t t)^{1/2})\right]. \tag{4.1}$$

The displacement speed of the iso-$\overline{\xi}$ surface is then given by

$$S_{\overline{\xi}} \sim \left(\frac{x_1}{(D_t t)^{1/2}}\right)\left(\frac{D_t}{t}\right)^{1/2} \sim \mathrm{erf}^{-1}(2\overline{\xi} - 1)\left(\frac{D_t}{t}\right)^{1/2}. \tag{4.2}$$

The entrainment into the iso-$\overline{\xi}$ surface thus scales with $t^{-1/2}$ for stationary homogeneous turbulence. The shape of Γ_η in Fig. 1 is similar to that in (4.2), but Γ_η shows different time dependence from $S_{\overline{\xi}}$ in the time period of $\tau < 3.2$. Γ_η is expected to have the same scaling as in (4.2) in a late stage of mixing when the thickness of the scalar mixing layer

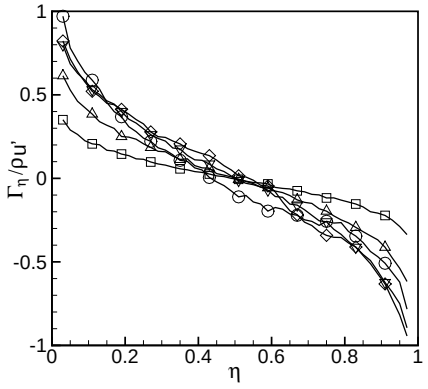

FIGURE 1. Total mass flux through the iso-η surfaces for conserved scalar mixing (square: $\tau = 0.21$, delta: $\tau = 0.54$, gradient: $\tau = 1.07$, diamond: $\tau = 2.14$, circle: $\tau = 3.21$).

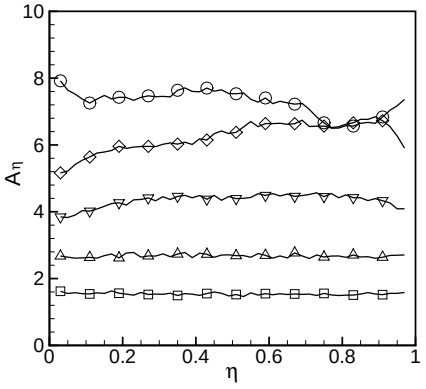

FIGURE 2. Wrinkled area ratio of the iso-η surfaces for conserved scalar mixing (see Fig. 1 for captions).

is much larger than integral length scale. The wrinkled area ratio A_η, at the same time instants as in Fig. 1, is shown in Fig. 2. A_η increases with time for $\tau < 3.2$, while it has weak dependence on η. This may have some implications for choosing the scalar threshold in the measurement of intermittency factor.

4.2. *Isothermal reaction fronts*

Figures 3(a) and 3(b) show instantaneous fields of the progress variable, C, at $\tau = 3.2$ and $\tau = 7.5$, respectively. At $\tau = 3.2$, the thickness of fronts has a range of length scales. The relatively thin fronts have a smaller thickness than do laminar fronts. The average thickness of the fronts is approximately equal to that of the laminar front at $\tau = 3.2$. At later time of $\tau = 7.5$, the fronts are much more thickened by small scale turbulence.

Figure 4 shows the turbulent burning velocity, (2.24), defined for various iso-C surfaces at several time instants. Note that S_T is negative at high values of ζ at the early stage of $\tau = 1.7$. It then increases for all ranges of ζ until $\tau = 4.28$. The iso-surfaces for lower values of ζ propagate faster than those for higher values of ζ at $\tau < 4.28$. This implies that the reaction fronts are being thickened on average. In the stationary propagation stage, $\tau > 6$, S_T should be equal for all values of ζ, although the numerical results show some fluctuations.

Figure 5 shows average local propagation speed of the iso-C surfaces, $S_T/(A_T S_L)$. At $\tau = 1.07$, the average mass flux per unit surface area is much greater than the laminar value S_L for small values of ζ, while it is small and even negative for large values of ζ. During the transient stage of $2 < \tau < 5$, the front propagation speed is close to the laminar one in the reaction zone. Iso-C surfaces for the pre-reaction zone propagate faster, while those for the post-reaction zone propagate slower than does the laminar one during this period. In the stationary propagation stage, the propagation speed of iso-C surfaces is slightly higher than the laminar one for all range of ζ.

4.3. *Premixed flames*

Figure 6 shows the conditional diffusion M_ζ for the cases PF1 and PF2. M_ζ closely follows the laminar flame value inside the flame brush for both cases. M_ζ is lower than

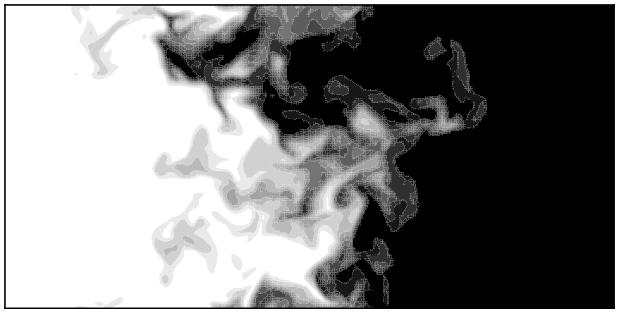

(a)

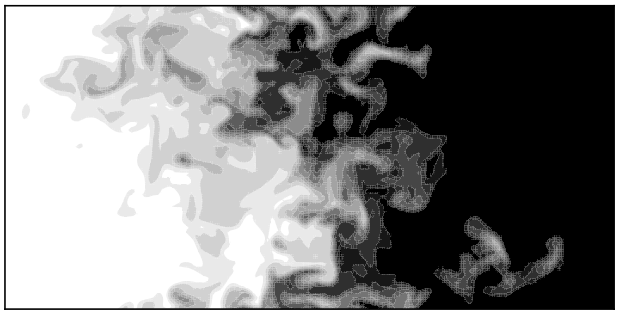

(b)

FIGURE 3. Instantaneous C-fields for isothermal reaction fronts (a) $\tau = 3.2$ (b) $\tau = 7.5$

the laminar flame value at the leading edge, while it is higher than the laminar flame value at the trailing edge. For PF2, the departure from the laminar flamelet behavior is more significant at the leading edge.

Figure 7 shows the apparent burning rate per unit volume R_ζ and the surface density function $\overline{\Sigma}_\zeta$ for the cases PF1 and PF2. Most burning occurs inside the flame brush. R_ζ decreases with ζ near the leading edge, while it increases with ζ near the trailing edge. Near the leading edge, the iso-C surfaces with $\zeta < 0.1$ propagate faster than the laminar front, while those with $\zeta > 0.1$ propagate more slowly than the laminar front. Iso-C surfaces propagate faster than the laminar front for all range of ζ near the trailing edge.

Figure 8 shows the turbulent burning velocity defined for various iso-C surfaces, S_T, and the total wrinkled area, A_T, for the cases PF1 and PF2. S_T and A_T show a dependence on ζ for both cases. For the case PF1, the turbulent burning rate normalized by the laminar one, S_T/S_L, is larger than A_T for $\zeta < 0.5$, which indicates that iso-C

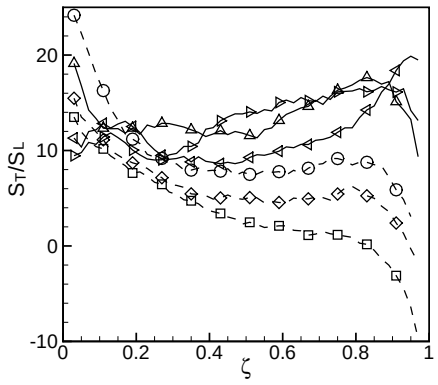

FIGURE 4. Turbulent burning velocity for isothermal reaction fronts (square: $\tau = 1.07$, diamond: $\tau = 2.14$, circle: $\tau = 4.28$, delta: $\tau = 6.43$, right triangle: $\tau = 7.5$, left triangle: $\tau = 8.57$; solid lines denote the stationary state; dashed lines denote the transient state)

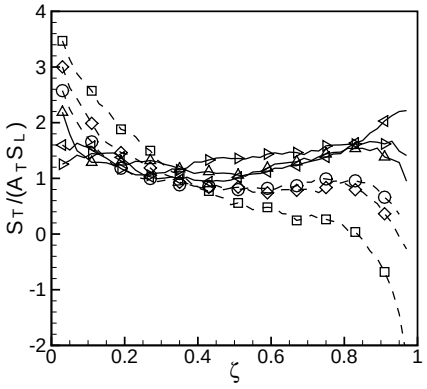

FIGURE 5. Average local propagation speed of the iso-C surfaces for isothermal reaction fronts (See Fig. 4 for captions)

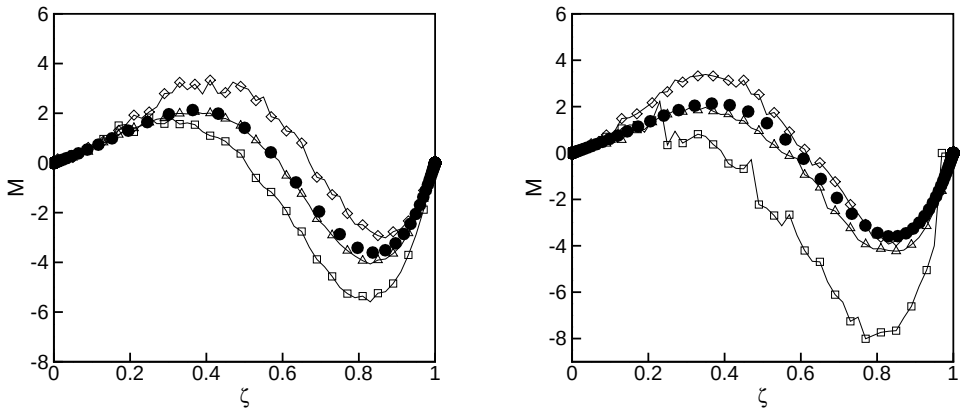

(a) PF1 (b) PF2

FIGURE 6. Conditional diffusion (circles: laminar value, square: leading edge, delta: flame brush center, diamond: trailing edge; $\tau \approx 4$, normalized by the laminar flame time scale).

surfaces for low values of ζ propagate faster than the laminar flame on average. For the case PF2, S_T/S_L is higher than A_T for $\zeta < 0.1$, while it is lower than A_T for $\zeta > 0.1$.

5. Discussion

The entrainment in turbulent jets and mixing layers can be measured by Γ_η. In the axisymmetric jet, for example, Γ_η is evaluated by integration of R_η along a radial direc-

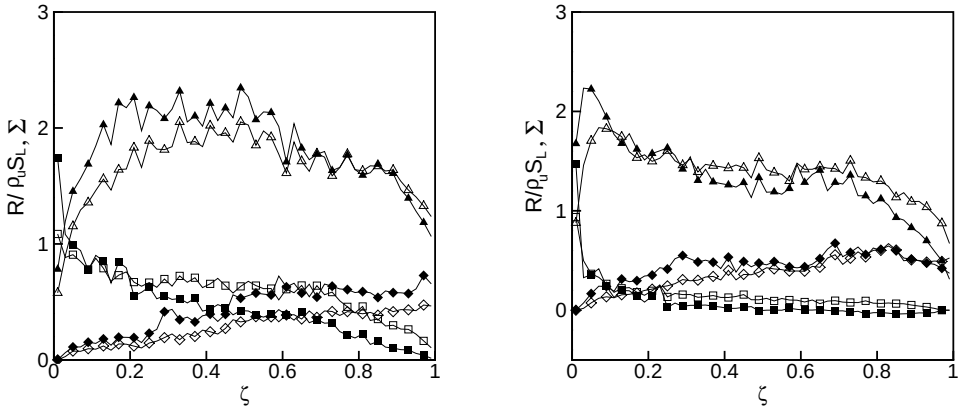

(a) PF1 (b) PF2

FIGURE 7. Mass flow rate per unit volume and surface density function for premixed flames (filled symbols: $R_\zeta/(\rho_u S_L)$, empty symbols: $\overline{\Sigma}_\zeta$, square: leading edge, delta: flame brush center, diamond: trailing edge; $\tau \approx 4$).

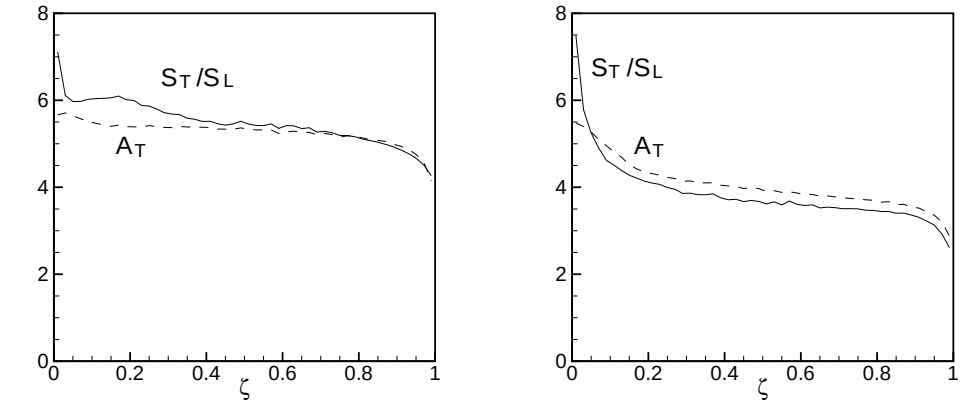

(a) PF1 (b) PF2

FIGURE 8. Turbulent burning velocity and wrinkled surface area ratio for premixed flames ($\tau \approx 4$).

tion, r, with the weighting factor of r/R_0, where R_0 is a characteristic radial dimension of the flow. The entrainment is then measured by Γ_η for η values that are low compared to the mean mixture fraction on the centerline. In the stationary axisymmetric jet, the axial variation of the mass flow rate through the area occupied by the fluid mixture with

$\xi > \eta_0$ on the $r - \theta$ plane is given by

$$\frac{dQ_{\eta_0}(z)}{dz} = 2\pi\Gamma_{\eta_0}(z), \tag{5.1}$$

where z is the axial coordinate.

In turbulent premixed flames, the apparent burning rate R_ζ can be integrated along the path normal to the mean scalar contours. This gives the turbulent burning velocity S_T, which depends on the value of ζ as well as on the location of the integration path. If the flame brush is statistically stationary and one-dimensional, the turbulent burning velocity does not depend on the value of ζ chosen. This single value of the turbulent burning velocity is the same as the mean fluid velocity in the cold boundary, the so-called turbulent flame speed in that case. During the developing phase of the one dimensional flame, S_T shows dependence on ζ when the local flame fronts are disturbed by turbulence. In practical flames and most laboratory flames, there is divergence in the flow, and the turbulent burning velocity can depend on the value chosen for ζ.

While conserved scalar mixing can be considered as the zero Da case, for which the diffusion layers are continuously broadened for thin enough initial layer thickness, it does not describe behavior in the limiting case of $Da \to 0$ and $t \to \infty$. The diffusion-reaction equation with constant diffusivity has an asymptotic propagating solution at $t \to \infty$ with some restrictions on the reaction rate (Kolmogorov *et al.* 1937; Lipatnikov & Chomiak 2005). When the initial laminar fronts are subject to strong turbulence, i.e. in low Da limit, the initial increase of the reactant consumption speed is primarily determined by turbulent transport. The initial propagation characteristics of the iso-surfaces of the progress variable are then similar to those of the conserved scalar. During the transient period, the brush thickness increases, while the scalar gradients in the brush decrease. A stationary state is reached when the steepening of scalar gradients by chemical reactions is balanced with mitigation of scalar gradients as a result of turbulent mixing. To the authors' knowledge, in contrast to the isothermal reaction front propagation in stationary homogeneous turbulence in the low Da limit, the existence of the stationary propagation state in turbulent premixed flames has not been demonstrated yet.

Negative burning velocity can occur when turbulent mixing is much stronger than chemical reactions. Subject to the compressive strain that is generated by large scale velocity structures, the reaction fronts are thinned and diffusive effects can be stronger than reaction ones for the whole range of ζ. The propagation of the fronts is then primarily governed by the diffusion process in the thin layers, and the negative burning velocity can occur for high values of ζ. When the fronts are disturbed by small scale turbulence, turbulent mixing in the fronts is enhanced due to turbulent folding and stretching. The fronts are then thickened. Small scale turbulence increases the propagation speed for low values of ζ, whereas it decreases that for high values of ζ, i.e. $\zeta \approx 1$.

In the thin reaction zone regime of turbulent combustion, the preheat zone is disturbed by small scale turbulence, while the reaction zone remains intact. Small scale turbulence then increases the diffusive transfer in the preheat zone. However, this does not necessarily mean that the mass flux into the reaction zone increases. According to the present results, the increase in the iso-surface propagation speed is more effective for lower values of ζ. Enhanced turbulent transport in the preheat zone can, therefore, thicken the preheat zone itself without significantly affecting the mass flux into the reaction zone. This situation is more likely to occur in turbulent premixed flames than in isothermal reaction fronts, since increased viscosity and/or dilatation effects tend to prevent small scale turbulence from entering into the reaction zone.

For turbulent premixed flames that are in the wrinkled laminar flamelet regime, the value of M_ζ is close to that in a planar, unstrained laminar flame. For significant amounts of wrinkling, the radius of curvature of the flame front can become of the same order as the thickness of the instantaneous flame front. The dependence of M_ζ on the locations of the flame brush in Fig. 6 is primarily due to these curvature effects. For the low Da case, PF2, turbulent premixed flames have more significant effects of small scale turbulence on the structure of the instantaneous flame front near the leading edge. The form and values of M_ζ are significantly influenced by small scale turbulence in Fig. 6. The turbulent burning velocity depends on the choice of ζ in these cases. The effects of the curvature are more evident near the leading and trailing edges.

In contrast to the progress variable, the iso-surfaces of the density may be used to identify the flame fronts in the low Mach number limit. From the continuity equation we have

$$\frac{D\rho}{Dt} = -\rho\nabla\cdot\mathbf{U}. \tag{5.2}$$

This yields

$$R_\kappa(\mathbf{x},t) = -\langle\rho^2\nabla\cdot\mathbf{U}|\kappa\rangle P_\rho(\kappa) = -\langle\nabla\cdot\mathbf{U}|\kappa\rangle\kappa^2 P_\rho(\kappa), \tag{5.3}$$

$$R_\nu = -R_\kappa = \langle\nabla\cdot\mathbf{U}|\kappa\rangle P_v(\nu), \tag{5.4}$$

where κ is the sample space variable for ρ and $v = 1/\rho$ is the specific volume with sample space variable ν. Note that R_κ values will be negative for flows with positive dilatation, because positive values imply flow across the iso-surface in the direction of increasing ρ. It is seen that for a premixed turbulent flame the apparent burning rate is directly proportional to the conditional average dilatation. The conditional average dilatation has been shown to be important in the structure of turbulent premixed flames (Swaminathan *et al.* 1997). The turbulent flame speed may be defined by integration of (5.3) as in (2.24).

It may be noted that the transport equation for the composition PDF, $P(\varphi;\mathbf{x},t)$, may be written (Pope 1990; Pope 2004) as

$$\frac{\partial\langle\rho|\varphi\rangle P_\phi}{\partial t} + \nabla\cdot(\langle\rho\mathbf{U}|\varphi\rangle P_\phi) = -\frac{\partial R_\varphi}{\partial\varphi}. \tag{5.5}$$

It is seen that the rate of change at a point plus the divergence of the convective flux is balanced by the negative of the rate of change in composition space of R_φ, the mass flux through the surface per unit volume.

6. Conclusions

A novel diagnostic method for characterization of iso-surface propagation in turbulent flows is proposed and applied to conserved scalar mixing, isothermal reaction fronts and turbulent premixed flames. The method is based on the concept of the apparent burning rate, i. e. the mass flow rate per unit volume through the iso-surfaces of a scalar. The expressions of the entrainment rate for conserved scalar mixing and the turbulent burning velocity for turbulent premixed flames are obtained by a line integration of this quantity. In contrast to the previous ones, the proposed expressions consider the dependence on a particular value of the scalar to better characterize the propagation of iso-scalar surfaces. Direct numerical simulation data for conserved scalar mixing and reaction front propagation in stationary homogeneous turbulence and one dimensional turbulent premixed flames are analyzed using the proposed method. The entrainment rate in the conserved scalar mixing case has a skew-symmetric profile and shows sensitivity to

a threshold value. It is shown that small scale turbulence more effectively increases the propagation speed of the iso-scalar surfaces for lower values of the progress variable in isothermal reaction fronts and premixed flames. The propagation speed for high values of the progress variable $C \approx 1$ is, however, lowered by the turbulent mixing. The negative propagation of the iso-surfaces can occur for high values of the reaction progress variable when the reaction fronts are subject to strong turbulence.

REFERENCES

Candel, S. M. & Poinsot, T. J. 1973 Flame stretch and the balance equation for flame area. *Combust. Sci. Tech.* **70**, 1-15.

Damköhler, G. 1940 Der einflußder Turbulenz auf die Flammengeschwidigkeit in Gasgemischen. *Z. Electrochem* **46**, 601-652.

Gibson, C. H. 1968 Fine structure of scalar fields mixed by turbulence. I. Zero-gradient points and minimal gradient surfaces. *Phys. Fluids.* **11**, 2305-2315.

Kennedy, C. A., Carpenter, M. H. & Lewis, R. M. 2000 Low-storage, explicit Runge-Kutta schemes for the compressible Navier-Stokes equations. *Appl. Nume. Math.* **35**, 177-219.

Klimenko, A. Y. & Bilger, R. W. 1999 Conditional moment closure for turbulent combustion. *Prog. Energy Combust. Sci.* **25**, 595-687.

Kolmogorov, A. N., Petrovskii, I. G. & Piskunov, N. S. 1937 A study of the diffusion equation with a source term for application to a biological problem. *Bull. Moscow State Univ. Ser. A* **1**, 1.

Lele, S. K. 1992 Compact finite difference schemes with spectral-like resolution. *J. Comp. Phys.* **103**, 16-42.

Lipatnikov, A. N. & Chomiak, J. 2005 Self-similarly developing, premixed turbulent flames: A theoretical study. *Phys. Fluids.* **17**, 065105.

Lundgren 2003 Linearly forced isotropic turbulence. *Annual Research Briefs 2003*, Center for Turbulence Research,NASA Ames/Stanford Univ., 461-473.

Poinsot, T. J. and Lele, S. K. 1992 Boundary conditions for direct numerical simulations of compressible viscous flows. *J. Comp. Phys.* **101**, 104-129.

Pope, S. B. 1988 The evolution of surfaces in turbulence. *Int. J. Eng. Sci.* **28**, 445-469.

Pope, S. B. 1990 Computation of turbulent combustion: progress and challenges. *Proc. Combust. Inst.* **23**, 591-612.

Pope, S. B. 2004 Private communication

Rosales, C. & Meneveau, C. 2005 Linear forcing in numerical simulations of isotropic turbulence: Physical space implementations and convergence properties. *Phys. Fluids.* **17**, 095106.

Swaminathan, N., Bilger, R. W. & Ruetsch, G. R. 1997 Interdependence of the instantaneous flame front structure and the overall scalar flux in turbulent premixed flames. *Combust. Sci. Tech.* **128**, 73-97.

Trouve, A. & Poinsot, T. J. 1994 The evolution for the flame surface density. *J. Fluid Mech.* **278**, 1-26.

Vervisch, L., Bidaux, E., Bray, K. N. C. & Kollmann, W. 1995 Surface density function in premixed turbulent combustion modeling, similarities between probability density function and flame surface approaches. *Phys. Fluids.* **7**, 2496-2503.